Available online at www.sciencedirect.com
SCIENCE DIRECT
Thermochimica Acta 440 (2006) 1–6
thermochimica acta
www.elsevier.com/locate/tca

Thermal decomposition process of silver behenate

Xianhao Liu [a,b], Shuxia Lu [c], Jingchang Zhang [a,*], Weiliang Cao [a]

[a] *Institute of Modern Catalysis, The Key Laboratory of Science and Technology of Controllable Chemical Reactions of Ministry of Education, Beijing University of Chemical Technology, Beijing 100029, China*
[b] *Institute of Research and Development, China Lucky Film Corp., Hebei Baoding 071054, China*
[c] *College of Mathematics and Computer Science, Hebei University, Hebei Baoding 071002, China*

Received 15 June 2005; received in revised form 23 August 2005; accepted 26 August 2005
Available online 2 November 2005

Abstract

The thermal decomposition processes of silver behenate have been studied by infrared spectroscopy (IR), X-ray diffraction (XRD), combined thermogravimetry–differential thermal analysis–mass spectrometry (TG-DTA-MS), transmission electron microscopy (TEM) and UV–vis spectroscopy. The TG-DTA and the higher temperature IR and XRD measurements indicated that complicated structural changes took place while heating silver behenate, but there were two distinct thermal transitions. During the first transition at 138 °C, the alkyl chains of silver behenate were transformed from an ordered into a disordered state. During the second transition at about 231 °C, a structural change took place for silver behenate, which was the decomposition of silver behenate. The major products of the thermal decomposition of silver behenate were metallic silver and behenic acid. Upon heating up to 500 °C, the final product of the thermal decomposition was metallic silver. The combined TG-MS analysis showed that the gas products of the thermal decomposition of silver behenate were carbon dioxide, water, hydrogen, acetylene and some small molecule alkenes. TEM and UV–vis spectroscopy were used to investigate the process of the formation and growth of metallic silver nanoparticles.

Keywords: Silver behenate; Combined TG-MS analysis; Thermal analysis; Thermal decomposition process

1. Introduction

Silver alkane carboxylate can be considered as inorganic–organic hybrid materials due to the structure of inorganic layers (the carboxylate groups and the silver ions) alternating with an organic layer (the double layers of alkyl chains) [1]. In the last few years, increasing attention has been paid to the structure and thermal behavior of silver carboxylates [1–4]. Silver salts of the long-chain fatty acids are used as the silver source in thermographic and photothermographic materials [5–8]. The most often used silver fatty acids in thermographic and photothermographic materials are silver behenate, silver stearate, or a mixture thereof [5–8].

Silver alkane carboxylate was reported to have a layered structure [9,10]. The knowledge of the thermal behavior of the silver carboxylates is of importance for an understanding of the thermographic process. Silver carboxylate does not simply melt in one step upon heating, but it undergoes a series of phase transitions before it melts with thermal decomposition [11,12]. As early as in 1886, Iwig and Hecht reported that silver butanoate is thermally decomposed into butanoic acid, carbon dioxide, carbon and metallic silver: $8C_3H_7COOAg \rightarrow 8Ag^0 + 7C_3H_7COOH + CO_2 + 3C$ [13]. Griffin et al. reported the thermal decomposition reaction mechanism of silver acetate [14]. The decomposition reaction they proposed is $2CH_3COOAg \rightarrow 2Ag^0 + CH_3COOH + CO_2 + H_2 + C$. Binnemans et al. [4] had proposed the decomposition of silver behenate is $2CH_3(CH_2)_{20}COOAg \rightarrow 2Ag + CO_2 + CH_3(CH_2)_{20}COOH + CH_3(CH_2)_{18}CH{=}CH_2$. The above authors found that the main decomposition products of the silver alkanoates were metallic silver and corresponding alkanoic acid, but they were not able to detect gas products during the thermal decomposition process. Although the presence of silver metal and alkanoic acid can be confirmed by XRD measurement and IR spectroscopy [15,16], respectively, the reported actual gas products at high temperatures are only a matter of conjecture.

To develop technologically relevant inorganic–organic hybrid materials, the whole thermal decomposition process must

* Corresponding author. Tel.: +86 10 64434904; fax: +86 10 64434898.
E-mail address: zhangjc1@mail.buct.edu.cn (J. Zhang).

0040-6031/$ – see front matter © 2005 Published by Elsevier B.V.
doi:10.1016/j.tca.2005.08.030

be known for their applications. In this paper, the detailed thermal behavior and decomposition process of silver behenate have been investigated by X-ray diffraction (XRD), Fourier transform infrared spectroscopy (FT-IR) and thermal analysis (TG-DTA). In order to confirm the species transported in the gas phase at different temperatures, the thermal decomposition intermediate gas products of silver behenate will be discussed by the combined TG-MS. Moreover, the thermal formation and growth of metallic silver nanoparticles will be characterized using TEM and UV–vis spectroscopy.

2. Experimental

2.1. Synthesis

All chemicals were purchased from commercial sources and used as received. The sodium behenate solution was prepared by firstly dissolving behenic acid in water-tert butyl alcohol mixing solvent at 80 °C, and then 0.25 mol L^{-1} sodium hydroxide solution was added with stirring at 1500 rpm. The molar ratio of behenic acid and sodium hydroxide was 1:1. Subsequently, the mixture was left being stirred for 1 h at 80 °C to obtain a solution of sodium behenate. Water-tert butyl alcohol mixed solvent, 5% (w/w) dodecylbenzene sulfonic acid sodium solution, tributyl phosphate and 3.0 mol L^{-1} silver nitrate solution were added with stirring into a reaction vessel. To enhance monodispersibility of grains and eliminate the formation of bubbles, dodecylbenzene sulfonic acid sodium and tributyl phosphate were added into the preparation process, respectively. The whole amount of the aforementioned sodium behenate solution and the equivalent mole amount of 3.0 mol L^{-1} aqueous silver nitrate solution were added at constant flow rates into the reaction vessel with fast stirring at 30 °C. After additions, the solution was stirred for 40 min at the same temperature and stirring rate. Subsequently, the white precipitate was filtered, and thoroughly washed with alcohol and distilled water until electric conductivity of the filtrate became less than 100 μS cm^{-1}. Finally, the white silver behenate was dried for 24 h in vacuum. The purity of the silver behenate was checked by C, H elemental analysis (% calc./found: C 59.05/59.04, H 9.69/9.67).

2.2. Characterization

The XRD patterns of powder sample were recorded on a Rigaku D/Max 2500 X-ray diffractometer using Cu $K\alpha_1$ (1.5406 Å) radiation operated at 40 kV and 200 mA for a 2θ angular range from 3° (2θ) to 50° (2θ) with a stepsize of 0.02° (2θ).

Infrared spectra were measured using a Bruker Vector 22 spectrometer. Pure KBr was used as the background. The proportion of KBr and sample was 1:0.015.

TG-DTA was performed on Pyris Diamond (Perkin-Elmer). The analyse was conducted in nitrogen atmosphere (100 mL min^{-1}) between 25 and 600 °C. Sample of 10 mg was put in a Pt cell and heated at a constant rate of 10 °C min^{-1}. MS spectra were measured on ThermostarTM (InProcess Instruments). The analysis was carried out in helium atmosphere (100 mL min^{-1}) between 25 and 600 °C.

Transmission electron microscopic (TEM) photographs of metallic silver nanoparticles were taken on a JEM-1200 EX-II (JEOL) microscope.

The UV–vis spectra of thermally decomposed samples at different temperatures were taken in toluene solvent with a Hitachi U-3000 spectrophotometer.

3. Results and discussion

3.1. The thermal behavior and decomposition processes of silver behenate

Fig. 1 shows a series of X-ray diffraction patterns of as-prepared silver behenate at various temperatures, ranging from 25 to 220 °C. In the small angle region a set of well-defined diffraction peaks is observed at 25 °C. These diffraction peaks belong to the (0 0 l) reflections. Such a diffraction pattern is consistent with a layer structure [4]. Each layer is separated from the other by twice the length of the alkyl chain [1]. It is noticeable from Fig. 1 that a well-produced progression of intense reflections is invariably seen below 140 °C. The presence of progressional reflections up to 120 °C indicates that the bilayer structural motif is sustained [16]. However, heating to 140–160 °C leads to substantial decreases of the layer reflections d(0 0 l) intensities, and the reflections are broadened. It can also be noticed from Fig. 1 that the XRD peak indexed as (0 0 l) abruptly decreases at 160 °C and cannot be identified at all at 190 °C. Instead, two new peaks are identified at 38.6° (2θ) and 44.3° (2θ) when the sample is heated above 190 °C. These peaks can be assigned to (1 1 1) and (2 0 0) reflections of metallic silver, showing that the major decomposition product of silver behenate is metallic silver.

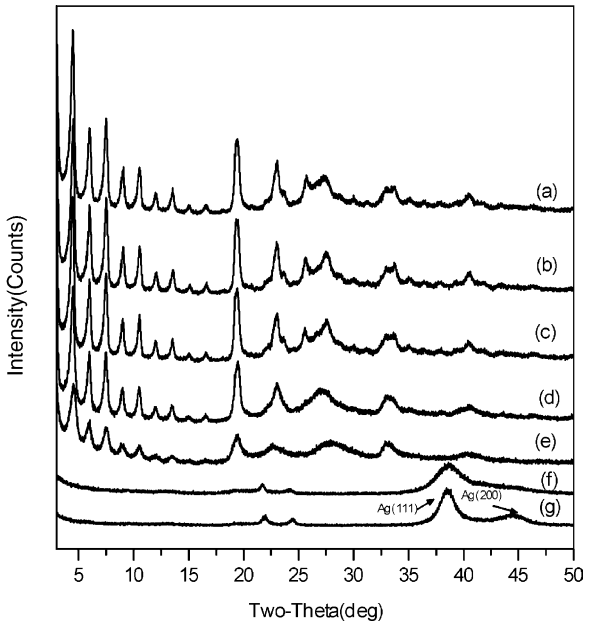

Fig. 1. XRD patterns of silver behenate at different temperatures: (a) 25 °C; (b) 100 °C; (c) 120 °C; (d) 140 °C; (e) 160 °C; (f) 190 °C; (g) 220 °C.

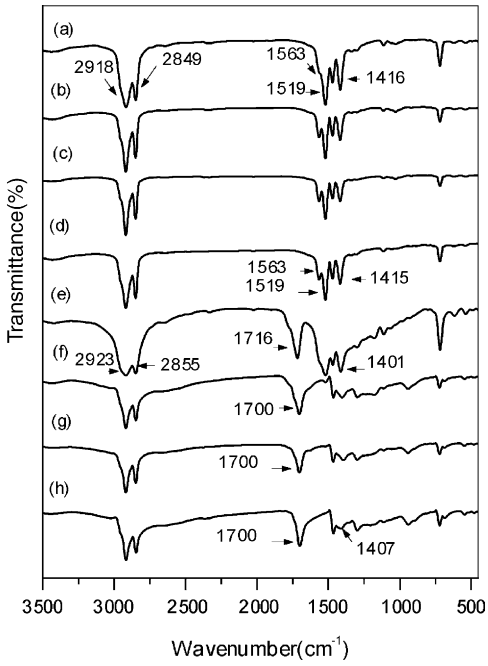

Fig. 2. Temperature-dependent IR spectra of silver behenate: (a) 25 °C; (b) 100 °C; (c) 120 °C; (d) 140 °C; (e) 160 °C; (f) 190 °C; (g) 220 °C; (h) 320 °C.

A variable temperature IR measurement is performed in order to obtain further information on the phase transition of silver behenate. Fig. 2 presents a series of IR spectra obtained as a function of temperature for silver behenate. The high-frequency region from 2800 to 3000 cm^{-1} reveals the C–H stretching modes of the methyl and the methylene groups of silver behenate. The two intense bands at 2849 and 2918 cm^{-1} at 25 °C are assigned, respectively, to the symmetric ($\upsilon_s(CH_2)$, d^+) and the antisymmetric ($\upsilon_{as}(CH_2)$, d^-) stretching vibrations of the methylene groups. The d^+ and d^- modes usually lie in the narrow ranges of 2846–2850 $cm^{-1}$and 2915–2918 cm^{-1}, respectively, for all-trans extended chains and in the distinctly different ranges of 2854–2856 cm^{-1} and 2924–2928 cm^{-1} for disordered chains characterized by a significant presence of gauche conformers [16]. On this basis, the observed peak frequencies of 2849 and 2918 cm^{-1} suggest that the alkyl chains in silver behenate are in an all-trans conformational state at 25 °C. Regarding the d^+ and d^- modes, the peak positions in Fig. 2 are invariant from 25 to 140 °C. This implies that the initial all-trans conformational order of the alkyl chains is preserved up to 140 °C. Upon increasing the temperature, the d^+ and d^- modes shift toward higher frequencies reaching 2855 and 2923 cm^{-1}, respectively, at 160 °C. These results indicate that a premelting event is characterized by the formation of gauche conformers. Additionally, silver carboxylate provides a rare opportunity to observe the effect of temperature on the headgroup structure. Regarding this matter, it is informative that the $\upsilon_{as}(COO^-)$ peak at 1519 cm^{-1} is rather invariant up to 120 °C and then slightly changes at 140 °C and disappears at 190 °C. The present observation suggests that the alkyl chains of silver behenate were transformed from an ordered into a disordered state around 140 °C. On the other hand, the $\upsilon_s(COO^-)$ peak at 1416 cm^{-1} decreases from 25 up to 320 °C and shifts gradually toward lower frequency reaching 1407 cm^{-1}. These results indicate that the structure change of silver behenate occurs distinctly above 190 °C, while the υ(C=O) peak at 1716 cm^{-1} produces around 160 °C and the peak at 1700 cm^{-1} appears at 190 °C. In a word, not only the present observation suggests that a certain structural change takes place, but it is reasonable to presume that the type of bonding of carboxylate to silver changes as well. Additionally, the free behenic acid produced from 190 °C has been sustained up to 320 °C. It is very interesting that the alkyl chains assume fully extended all-trans conformation at higher temperatures [16] and the obtained metallic silver particles are passivated by behenic acid based on the analysis of XRD patterns. The IR analysis indicates that silver behenate is thermal stable below 120 °C, above which the structural change happens. The major products of the thermal decomposition are metallic silver and behenic acid from190 to 320 °C.

TG-DTA curves of as-prepared silver behenate are shown in Fig. 3. Three intense endothermic peaks at 138, 231, and 318 °C are observed. These peaks suggest that structural changes occurred distinctly around the three temperatures. The peak at 138 °C can be assigned to the structural transformation associated mainly with the disordering of the alkyl chains. The most intense endothermic peak at 231 °C can be attributed to the rapid thermal decomposition of silver behenate. The broad endothermic peak at around 318 °C suggests that the thermal decomposition intermediate products of silver behenate further decompose. Two weak endothermic peaks at 159 °C and 193 °C are observed. The endothermic peak at 159 °C should be assigned to the crystal phase transition of a mesophase to mesophase transition [14]. Above 159 °C, silver behenate starts to decompose. The endothermic peak at 193 °C should be attributed to the thermal decomposition of silver behenate. The observed exothermic stages at 460 and 510 °C can be rationalized as a result of silver

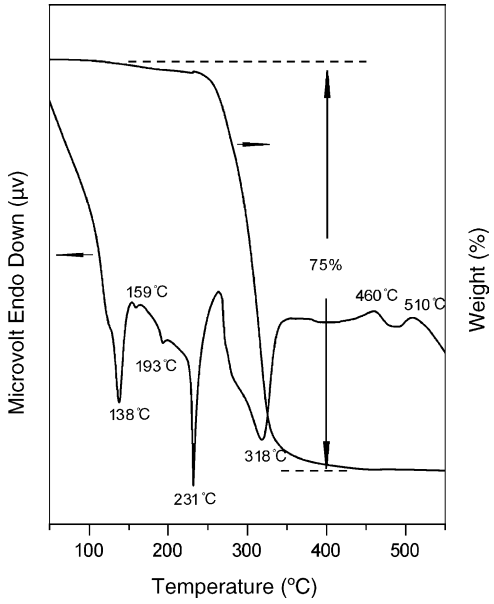

Fig. 3. TG-DTA curves of silver behenate.

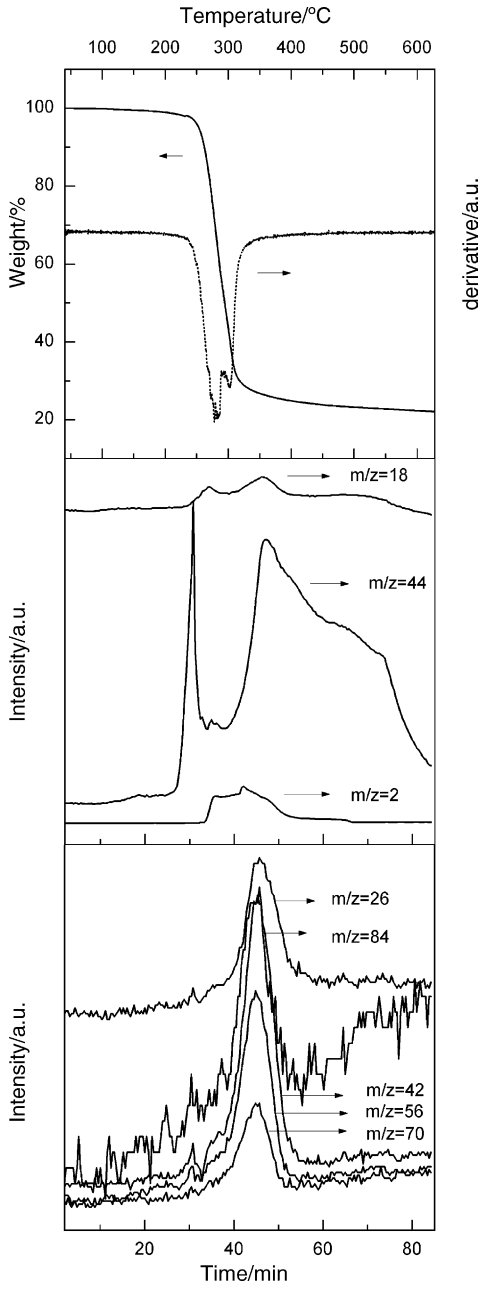

Fig. 4. TG-DTG plot and mass analyses of silver behenate.

cluster formation, and their further transformation to the metallic form.

Fig. 4 presents the TG-MS analysis of silver behenate. In Table 1 are the detailed characteristic *m*/*z* values of the analyzed different species, while the thermogravimetric plot shows three weight losses. Among the three, the first very small one centred at about 230 °C can be attributed mainly to the evolved gas of carbon dioxide, as confirmed by the following MS analyses. The *m*/*z* value of 44 is characteristic of carbon dioxide which indicates the carbon dioxide gas product begins to appear at about 230 °C. The *m*/*z* values of 18 and 2 are characteristics of water and hydrogen, respectively. These species at about 260 °C are the second thermal decomposition gas products. From the analysis of DTG curve, the first and second thermal decomposition processes are two overlapping stages that dissociate in the two subsequent processes. The third decomposition gas products appear in the temperature range centred at about 350 °C. The characteristic *m*/*z* values of the different species are as follows: 2(hydrogen), 44(carbon dioxide), 18(water), 26(acetylene), 42(propylene), 56(butene), 70(pentene) and 84(hexene). The mass loss commences at about 230 °C in the TG curve and concludes around 500 °C. The actual mass loss amounts to 75.0% from 230 to 500 °C, which is close to that calculated theoretically (75.8%). The residue from the remaining decomposition calculates to metallic silver, which agrees with its visual white appearance. So, it is well confirmed from TG-MS analysis of silver behenate that the final product of the thermal decomposition at high temperature (above 500 °C) is metallic silver.

Table 1
Selected mass-ions

Temperature (°C)	*m*/*z*	Assignment (fragments)
~230 °C	44	Carbon dioxide
~260 °C	2, 18	Hydrogen, water
~350 °C	2, 44, 18, 26, 42, 56, 70, 84	Hydrogen, carbon dioxide, water, acetylene, propylene, butene, pentene, hexene

3.2. The nature and morphology of silver nanoparticles

Lee et al. [16,17] ascertained from IR spectroscopy that the silver nanoparticles were passivated by stearates or perfluorocarboxylates. In this study, the major solid state products of the thermal decomposition of silver behenate from 190 to 320 °C are metallic silver and behenic acid. The heated silver behenates were rinsed thoroughly with methanol to remove possible impurities, and were then dispersed in toluene. Fig. 5 shows the TEM images and size distribution histograms of the samples taken after vaporizing the toluene solvent on the surface of the copper grid. The particle size distribution histograms in Fig. 5 were measured from an analysis of 350 particles (the equivalent circular grain diameter of each grain can be determined). The images reveal that the sizes of the nanoparticles are quite uniform with an average diameter of 7(2) nm at 190 °C and the size of the silver nanoparticles increases as the temperature increases. Meanwhile, more and more large silver nanoparticles with an average diameter of 10(2) nm are formed at 220 °C due to aggregation with increasing the temperature. For growth by Oswald ripening, aggregation and precipitation lead to a broad distribution. As a result, it is remarkable that the sizes of silver nanoparticles are uniform with an average diameter of 18(3) nm at 320 °C. However, more dramatic aggregation is observed as the heating temperature increases.

The formation of silver nanoparticles can be supported by the results of a UV–vis spectroscopic study. The UV–vis absorption spectra of the toluene solutions containing silver nanoparticles for samples formed at three different temperatures are shown in Fig. 6. For the samples at 190 °C and 220 °C, narrow absorption maxima are seen at 425 nm and 450 nm, respectively. In the case of the sample at 320 °C, the absorption maximum is red-shifted

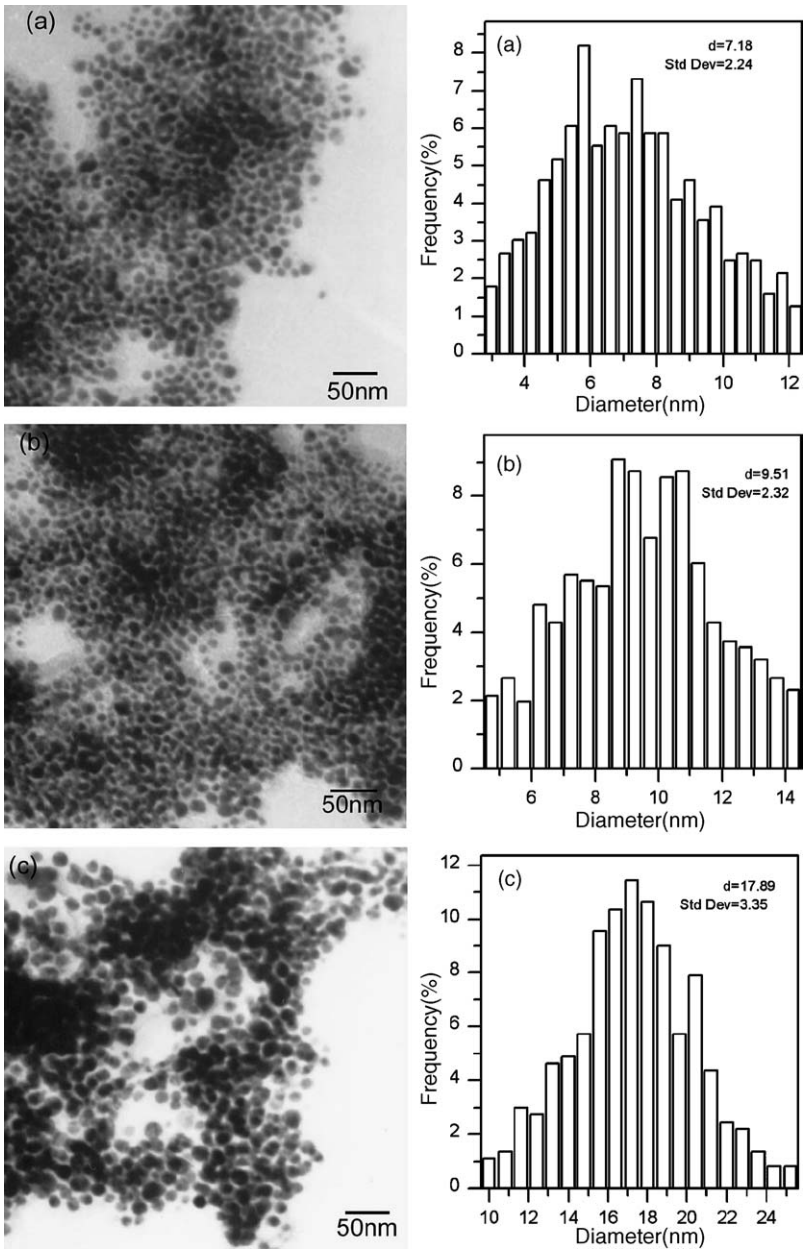

Fig. 5. TEM images and size distribution histograms of the obtained silver nanoparticles at different temperatures (a) 190 °C; (b) 220 °C; (c) 320 °C.

to 480 nm. Presumably, this is associated with the increase in the particle size. Absorption spectra of larger metal colloidal dispersions can exhibit broad bands in the UV–vis range due to the excitation of plasma resonances [18]. In addition, densely aggregation particles exhibit surface plasmon resonance features that are broadened considerably by dipole–dipole interactions and can have either red or blue-shifted excitation spectra compared with those of isolated particles [19].

3.3. Proposed reaction mechanism of thermal decomposition of silver behenate

The above results can be discussed by use of the following reaction mechanism for thermal decomposition of silver behenate. Andreev et al. [20] reported that metallic silver, carbon dioxide, the corresponding acid, and products of the organic radical reaction were produced upon heating long-chain silver carboxylates. The organic radicals were supposed to recombine with the formation of paraffins, or to undergo further reactions. The obtained products are most likely formed by free radical pathway by the pyrolysis of silver behenate. In our work, the thermal decomposition of silver behenate was observed to occur above 190 °C. The C=O stretching peak was clearly identified at ∼1700 cm^{-1} above 190 °C, which must have arisen from a free acid. Hydrogen atoms required for forming free acid are provided by the dehydrogenation reaction that may occur during the thermal decomposition of the organic moiety of silver behenate. The dehydrogenation of the hydrocarbon chains has been reported to be the representative reaction of such materials [21]. During the first transition at ∼230 °C, the

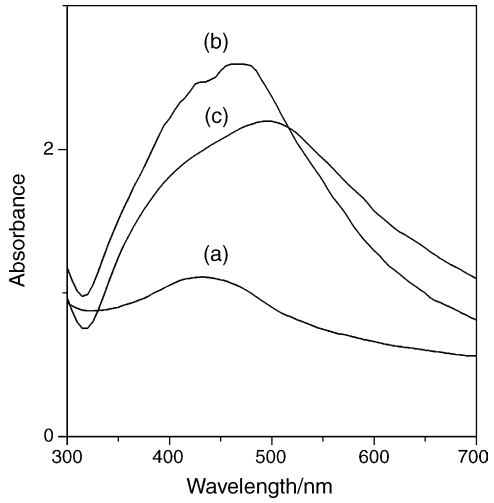

Fig. 6. Optical absorbance of silver nanoparticle/toluene solution of the heated sample (a) 190 °C; (b) 220 °C; (c) 320 °C.

TG-MS shows carbon dioxide evolving. The most probable thermal decomposition scheme for silver behenate may be: $2CH_3(CH_2)_{20}COOAg \rightarrow 2Ag + CO_2 + CH_3(CH_2)_{20}COOH + CH_3(CH_2)_{18}CH{=}CH_2$, which is in accordance to the reaction pattern proposed by Binnemans et al. As temperature increases, behenic acids condense to form anhydrides and expel water. The dehydrogenation of the hydrocarbon chains results in the formation of hydrogen. The characteristic *m*/*z* values at ∼260 and ∼350 °C conformed the presence of water and hydrogen, and the formation of acetylene and some small molecule alkenes due to the pyrolysis of silver behenate at ∼350 °C. In fact, the thermal decomposition of behenic acid occurs at ∼350 °C, and its thermal decomposition gaseous products are close to that of silver behenate, which are identified by the TG-MS of pure behenic acid.

4. Conclusions

These results analyzed by infrared spectroscopy (IR), X-ray diffraction (XRD), thermogravimetry–differential thermal analysis (TG-DTA) demonstrated that complicated structural changes took place with heating silver behenate, there were two distinct transitions. During the first transition at 138 °C, the alkyl chains of silver behenate were transformed from an ordered into a disordered state. During the second transition at 231 °C, a structural change took place indicating the decomposition of silver behenate. The major decomposition products were metallic silver and behenic acid. The combined TG-MS analysis showed that the intermediate gas products of the thermal decomposition of silver behenate were carbon dioxide, water, hydrogen, acetylene and some small molecule alkenes. The TEM and UV–vis results indicated that the formation and growth of silver nanoparticles were followed by ablation process due to Oswald ripening and reached the quite uniform particle distribution. As silver behenate was continuously heated up to 500 °C, the behenic acid-stabilized silver nanoparticles gradually lost organic moieties due to further thermal decomposition of behenic acid. The final product of the thermal decomposition was metallic silver.

References

[1] S.J. Lee, S.W. Han, H.J. Choi, K. Kim, Eur. Phys. J. D 16 (2001) 293.
[2] B.B. Bokhonov, L.P. Burleva, D.R. Whitcomb, M.V. Sahyun, Microsc. Res. Techniq. 42 (1998) 152.
[3] B.B. Bokhonov, L.P. Burleva, D.R. Whitcomb, M.L. Brostrom, J. Imaging Sci. Technol. 48 (2004) 1.
[4] K. Binnemans, R.V. Deun, B. Thijs, I. Vanwelkenhuysen, I. Geuens, Chem. Mater. 16 (2004) 2021.
[5] P.J. Cowdery-Corvan, D.R. Whitcomb, Handbook of Imaging Materials, A.S. Diamond, D.S. Weiss (Eds.), Marcel Dekker, Inc., New York, 2002, p. 473.
[6] M.R.V. Sahyun, J. Imaging Sci. Technol. 42 (1998) 23.
[7] P.M. Zavlin, A.N. Batrakov, P.Z. Velinzon, S.I. Gaft, L.L. Kuznetsov, J. Imaging Sci. Technol. 43 (1999) 540.
[8] I. Geuens, I. Vanwelkenhuysen, J. Imaging Sci. Technol. 43 (1999) 521.
[9] F.W. Matthews, G.G. Waren, J.H. Michell, Anal. Chem. 22 (1950) 514.
[10] R. Gilles, U. Keiderling, A. Wiedenmann, J. Appl. Crystallogr. 31 (1998) 957.
[11] N.F. Uvarov, N.F. Burleva, M.B. Mizen, D.R. Whitcomb, C.F. Zou, Solid State Ionics 107 (1998) 31.
[12] B.B. Bokhonov, L.P. Burleva, D.R. Whitcomb, Y.E. Usanov, J. Imaging Sci. Technol. 45 (2001) 259.
[13] F. Iwig, O. Hecht, Ber. Dtsch. Chem. Ges. 19 (1886) 238.
[14] R.G. Griffin, J.D. Ellett Jr., M. Mehring, J.G. Bullitt, J.S. Waugh, J. Chem. Phys. 57 (1972) 2147.
[15] S.J. Lee, S.W. Han, K. Kim, Chem. Commun. (2003) 212.
[16] S.J. Lee, S.W. Han, H.J. Choi, K. Kim, J. Phys. Chem. 106 (2002) 2892.
[17] S.J. Lee, S.W. Han, K. Kim, Chem. Commun. (2002) 442.
[18] P.V. Kamat, M. Flumiani, G.V. Hartland, J. Phys. Chem. B 102 (1998) 3123.
[19] R.P. Van Duyne, J.C. Hulteen, D.A. Treichel, J. Chem. Phys. 99 (1993) 2101.
[20] V.M. Andreev, L.P. Burleva, V.V. Boldyrev, I.Y. Mikhaliv, Izv. SO AN USSR, Serkhim. Nauk 2 (1983) 58.
[21] M.J. Blazso, B. Zelei, E. Jakab, J. Anal. Appl. Pyrol. 35 (1995) 221.